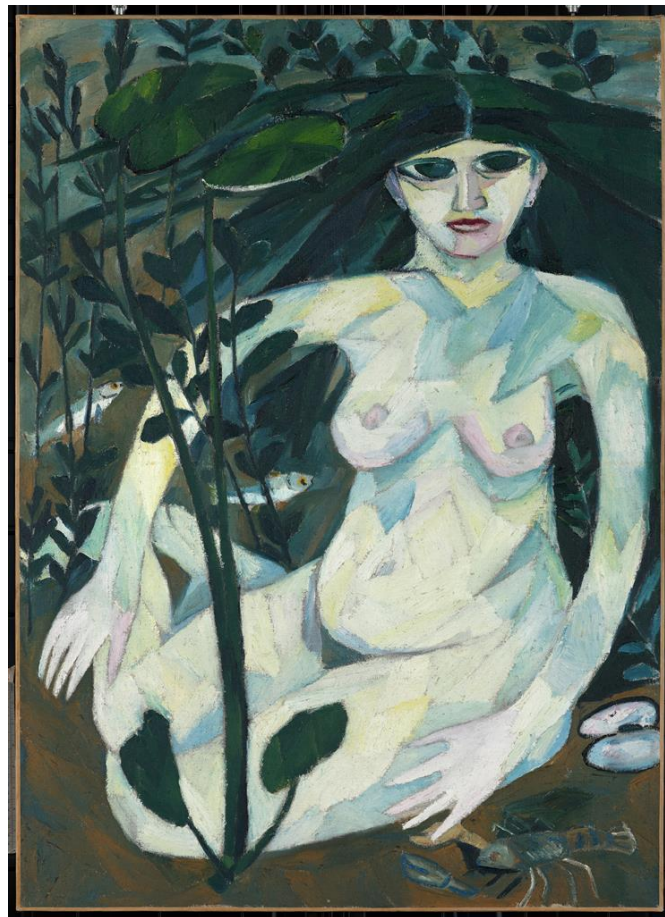


## ANALYTICAL REPORT

[Ref.: AAR0955.B / 8 May 2018]



*Rusalka (Water Nymph)*, 1908

Natalia Goncharova

Collection Museum Ludwig, Cologne, Inv. ML 1304

Art Analysis & Research Inc.  
Ground Floor West, 162-164 Abbey Street, London SE1 2AN  
T: +44 (0) 20 7064 1433  
VAT Reg. No. 252 4541 22

## Summary

A painting on canvas by Natalia Goncharova, *Rusalka (Water Nymph)*, with a proposed date of creation of 1908 (it is unsigned and undated), belonging to the Museum Ludwig (ML 1304) was examined and analysed by Art Analysis & Research, Ltd. in cooperation with the Museum, and funded through a grant from the charity The Russian Avant Garde Research Project (RARP). This artwork was assessed as part of a group of fourteen well-provenanced paintings by the Russian artist couple Natalia Goncharova and Mikhail Larionov, held in the collection of the Museum Ludwig. The goal set for this research was to investigate these paintings in order to characterise similarities and differences, with the goals of 1) providing detailed studies of specific paintings, 2) providing wider information on the artists' methods, 3) defining a blueprint for promising methodologies to develop further on other works by these artists and applying such information in support of a *catalogue raisonné*, and 4) creating the foundation for applying similar methodologies and techniques to other artists of the genre. To this end, each of the paintings are described in individual reports (as here) accompanied by a summary report under separate cover. The results of the program of examination, material analysis and technical imaging will be set out herein.

## Contents

Summary .....	2
Tables, Figures and Plates.....	4
A. Introduction.....	6
B. Examination, imaging and analysis of the images .....	7
B.1 Methodology .....	7
B.2 General observations .....	7
B.3 Imaging.....	8
B.3.i Photography with ultraviolet illumination .....	8
B.3.ii Surface conformation .....	8
B.3.iii Short-wave infrared (SWIR).....	9
B.3.iv X-radiography and weave analysis .....	10
C. Sampling and analysis .....	10
C.1 Introduction .....	10
C.2 Support .....	11
C.3 Radiocarbon dating.....	12
C.4 Ground.....	12
C.5 Underdrawing .....	12
C.6 Paint layers: Pigments .....	12
C.7 Paint layers: Binding media .....	13
C.8 Stratigraphy .....	13
D. Discussion of the findings .....	13
D.1 Support, ground and preparatory work .....	13
D.1.i The support .....	13
D.1.ii Priming.....	14
D.1.iii Underdrawing .....	14
D.2 Paint, pigments and binding media .....	15
D.2.i General observations.....	15
D.2.ii Paint: pigment and binding medium .....	16
D.2.iii Materials analysis and implications for dating .....	16
E. Conclusions .....	17
F. Acknowledgements.....	18
G. Appendices .....	19

App.1. Sampling and sample preparation .....	19
App.1.i Sampling .....	19
App.1.ii Cross-sectional analysis .....	20
App.2. Materials analysis summary results .....	20
App.2.i SEM-EDX, Raman microscopy and PLM analysis .....	20
App.2.ii Fourier Transform Infrared Spectroscopy-Attenuated Total Reflectance (FTIR-ATR) .....	22
App.2.iii Gas Chromatography Mass Spectrometry (GCMS) Analysis .....	23
App.2.iv Protein staining with SYPRO® Ruby .....	23
App.2.v Fibre Identification of the Canvas .....	23
App.2.vi Radiocarbon measurement .....	24
App.3. Imaging methods .....	26
App.4. Plates .....	27
App.5. Cross-sections .....	41

## Tables, Figures and Plates

Table App.1.i Samples taken for analysis .....	19
Table App.2.i Analytical results SEM-EDX, Raman Microscopy and PLM .....	20
Table App.2.ii Summary results from FTIR .....	22
Table App.2.iii Summary results from GCMS .....	23
Table App.2.iv SYPRO® Ruby stain results for 955.B, sample [3] .....	23
Table App.2.v Canvas fibre identification .....	23
Table App.2.vi.i Radiocarbon measurement .....	24
Figure App.2.vi.ii Radiocarbon determination. ....	25
Plate 1. Natalia Goncharova, Rusalka, 1908, collection Museum Ludwig: Inv. Nr. ML 1304. Recto, visible light .....	27
Plate 2. Natalia Goncharova, Rusalka, 1908, collection Museum Ludwig: Inv. Nr. ML 1304. Recto, UV light .....	28
Plate 3. Natalia Goncharova, Rusalka, 1908, collection Museum Ludwig: Inv. Nr. ML 1304. Recto, raking light. ....	29
Plate 4. Natalia Goncharova, Rusalka, 1908, collection Museum Ludwig: Inv. Nr. ML 1304. Recto, 3D laser scan. ....	30
Plate 5. Natalia Goncharova, Rusalka, 1908, collection Museum Ludwig: Inv. Nr. ML 1304. Verso, visible light .....	31
Plate 6. Natalia Goncharova, Rusalka, 1908, collection Museum Ludwig: Inv. Nr. ML 1304. Recto, SWIR image .....	32
Plate 7. Natalia Goncharova, Rusalka, 1908, collection Museum Ludwig: Inv. Nr. ML 1304. Recto, detail of SWIR image, contrast heightened. ....	33

Plate 8. Natalia Goncharova, Rusalka, 1908, collection Museum Ludwig: Inv. Nr. ML 1304. X-ray image.....	34
Plate 9.a Maps showing variation in canvas thread angle.....	35
Plate 9.b Histogram of vertical thread count readings.....	36
Plate 9.c Histogram of horizontal thread count readings.....	36
Plate 9.d Table of thread count data (threads per centimetre) .....	36
Plate 10.a Detail of canvas, recto, showing the exposed tabby weave canvas, upper right corner. ..	37
Plate 10.b Detail of the primed canvas. ....	37
Plate 10.c Detail of the canvas, recto, showing an example of the irregular thread inclusions. ....	37
Plate 11.a Microscopic detail of the underdrawing material. ....	38
Plate 11.b Microscopic detail recto; thin ground and underdrawing, loose fibres.....	38
Plate 11.c Microscopic detail of paint, showing plant husk fragments from the canvas. ....	38
Plate 12.a Detail of the underdrawing material.....	39
Plate 12.b Detail X-ray image, as 11.a.....	39
Plate 12.c Detail of paint, showing contouring of form in green (nose).....	39
Plate 13. Image showing approximate location of samples taken for materials analysis. ....	40
Plate 14. Cross section, Sample [3].....	41
Plate 15. Cross section, Sample [3].....	41
Plate 16. Cross section, Sample [3], stained with SYPRO® Ruby. ....	42
Plate 17. Cross section, Sample [5].....	42
Plate 18. Cross section, Sample [5].....	43

## A. Introduction

The painting known as *Rusalka* (*Water nymph*; **Plate 1**) by the artist Natalia Goncharova (1881-1962), a work on canvas measuring 1040 mm high by 740 mm wide, is now part of the collection of the Museum Ludwig, Cologne (Inv. ML 1304). It is unsigned and undated; a date of 1908 has been proposed for its creation. It has been examined as part of a larger technical study of fourteen paintings by Goncharova and Mikhail Larionov in the Museum Ludwig, as part of a project funded through a grant from the charity the Russian Avant Garde Research Project (RARP). The project goal has been to generate detailed technical profiles on authentic paintings by Goncharova and Larionov to expand the data available for art historical study and technical characterization of their work<sup>1</sup>; consequently, fourteen well-provenanced paintings by the Russian artist couple held in the collection of the Museum Ludwig were thoroughly examined and analysed<sup>2</sup>. The short-term goal of the project was to define a blueprint for promising routes of research to develop further on other works by these artists and with a long-term goal of contributing such information to support a technical *catalogue raisonné*; these recommendations are laid out in a summary report<sup>3</sup>.

The information in this report therefore provides a detailed technical and material account of the painting. In addition, this material is considered in light of the conservation history and provenance information relating to the painting, held by the Museum Ludwig; the supplementary reports produced by Verena Franken in the course of her work on the RARP project summarises this material<sup>4</sup>. Some of the information concerning examination of the paintings has been included here, as relevant, as are a representative selection of the extensive documentation photographs she made.

The structure of this report is as follows. First, the primary findings of the visual examination and technical imaging will be described in **Section B**.

Materials analysis on micro-samples taken for pigment and binding medium identification and cross-sections is described in **Section C**.

<sup>1</sup> There is limited specific information available. This includes: Rioux, J.-P.; Aitken, G.; Duval, A. 'Étude en laboratoire des peintures de Gontcharova et Larionov', pp. 220-223. In: *Nathalie Gontcharova, Michel Larionov* [exh. cat.], Éditions du Centre Pompidou : Paris (1995). Rioux, J.-P.; Aitken, G.; Duval, A. 'Matériaux et techniques des peintures de Nathalie S. Gontcharova et Michel F. Larionov du Musée national d'art moderne', *Techne* 8 (1998) 7-32. Gallone, A. 'Œuvres de Michel Larionov et Nathalie Gontcharova: Analyse de la Couleur', *Le dessin sous-jacent la technologie dans la peinture: Colloque XI 14-16 septembre 1995*, R. Van Schoute and H. Verougstraete (eds), Louvain-la-Neuve (1997) pp. 137-141, Pl. 74-76.

<sup>2</sup> These include: Natalia Goncharova: *Paysage de Tiraspol (Tiraspol Landscape)*, 1905, ML 01483; *Rusalka*, 1908, ML 1304; *Still Life with Tiger Skin*, 1908, ML 1305; *The Jewish Family*, 1912, ML 1369; *The Orange Seller*, 1916, ML 1484; *Portrait of Larionov*, 1913, ML 1319.

Mikhail Larionov, *Still Life with Coffee Pot*, c. 1906, ML 01486; *Still Life*, c. 1907/1912, ML 1487; *Still Life with a Crayfish (Nature morte à l'écrevisse)*, c. 1907, ML 1331; *Portrait of a Man (Anton Beswal)*, c. 1910, ML 1306; *Rayonism, Red and Blue (Beach)*, 1911, ML 1333; *Saucisson et maquereau rayonnists (Rayonistic Sausage and Mackerel)*, 1912, ML 1307; *Venus*, 1912, ML 1332; *Rayonistic Composition*, inscribed 1916, ML/Z 211/134.

<sup>3</sup> *Summary Report of the RARP Goncharova/Larionov Project, with the Museum Ludwig*, Art Analysis & Research Inc. (2017).

<sup>4</sup> See reports: *AAR0955.A ML 1304 Conservation*, Franken, V. 'Report on the examination of the painting *Rusalka* (1908) by Natalia Goncharova' (2017a) and *AAR0955.A ML 1483 Archives*, Franken, V. 'Report on the content of the Museum Ludwig archives, concerning the painting *Rusalka* (1908) by Natalia Goncharova' (2017b).

Inferences drawn regarding the painting on the basis of these investigations will be discussed in **Section D**.

The methodologies and protocols used in each case may be found described in the general **Protocols** supplement, appended to this series of reports.

## **B. Examination, imaging and analysis of the images**

### **B.1 Methodology**

The painting was initially examined visually under normal lighting conditions and with ultraviolet light (UV), then with a stereo binocular microscope.

A range of technical imaging techniques were also employed (**Appendix 3**), generating a variety of images and imaging datasets<sup>5</sup>. These are presented as follows:

- High-resolution visible colour (**Plates 1, 5**);
- UV luminescence (**Plate 2**);
- Oblique illumination (**Plate 3**);
- 3D laser surface scanning (**Plate 4**);
- Short-wave infrared (SWIR), 1600-2500nm (**Plates 6, 7**);
- X-radiography (**Plate 8**).

Additionally, weave analysis (including thread counting) was conducted on the basis of the X-radiograph (**Plates 9.a-c**). Some exemplar images recorded as part of the surface microscopy and macrophotography are also reproduced here (**Plates 10-12**).

The imaging revealed a range of aspects regarding the use of materials, structure and technique of production of the painting that are complementary to the visual observations made. Consequently, specific observation will be made to each in this section regarding the interpretation of these specific forms of analysis, while a summary overview in the context of the painting technique is presented in **Section D**, below.

### **B.2 General observations**

The painting is executed on a rough canvas, which has been lined. Its tacking margins were largely cut away during this process and the edges finished with paper tape, so that only the recto of the artwork could be studied. Nor is it on its original stretcher, having been re-stretched onto a newer secondary support, a stretcher with two crossbars and 12 keys (**Plate 5**). The painting is in good

---

<sup>5</sup> Additionally, a visible-NIR multispectral dataset was collected to examine its suitability for study of paintings of Goncharova and Larionov. As it did not offer information significantly different or superior to that derived by the SWIR imaging, this has not been otherwise reproduced or further analysed here but is available for extramural studies in the future.



condition, with mostly minor, localised retouching. The most significant damages are a horizontal crease in the canvas (about centre). The painting is not varnished.

### B.3 Imaging

Each form of imaging offers different types of insight into the various material aspects of the painting. The most relevant are introduced, in brief, here.

#### *B.3.i Photography with ultraviolet illumination*

Excitation by ultraviolet (UV) light can induce luminescence<sup>6</sup> in some materials, commonly seen as a weak re-emission of light in the visible region. Many natural varnishes have this property, emitting a characteristic weak greenish luminescence. While some pigments (notably zinc white and certain 'lake' pigments) are also active in this way, paints otherwise often do not luminesce. Because of the luminescence of varnishes, which are typically applied as a continuous coating across the surface of a painting, this can provide a means of determining if any disturbance has occurred, such as partial cleaning of the surface or addition of later restoration, where the changes show in contrast to the luminescent areas. Consequently, UV light is commonly used to reveal the presence of retouching. When paintings are not varnished, as is the case here, differences between the colour of the luminescence of the different paints and any added retouching paints may also indicate later stages of intervention (as here; **Protocol 3.2** and **Plate 2**).

In the UV image of this work, no evidence for a varnish is visible. Retouching along the horizontal crease running along the centre of the painting is clearly visible. No strong luminescence was noted from any of the original paints.

#### *B.3.ii Surface conformation*

Two techniques for examination of the surface structure of the painting were used: photography under oblique illumination and 3D laser scanning. While the former may be the more familiar of the two as a physical examination technique, both essentially provide a means of elucidating paint texture and object deformations, either by recording shadowing, or through direct measurement of surface height. Of the two, 3D laser scanning offers important advantages in terms of being more replicable in the future (to support longer-term conservation assessments for example) and as a numerical dataset that can be studied visually and algorithmically for diagnostic features of technique. Imaging of the painting using oblique illumination, as well as 3D laser surface scanning (see **Protocol 3.3**), served to reveal two kinds of textural features that are particularly evident in this painting.

---

<sup>6</sup> Commonly referred to as 'UV fluorescence', the word *luminescence* is used here as a broader term that may encompass not only fluorescence phenomena (prompt re-emission of light), but also phosphorescence (slow re-emission of light due to transition via forbidden quantum states). In both cases emission is typically at longer wavelengths than the excitation; here, the excitation is in the UV to blue part of the spectrum (hence 'UV'; in practice, so-called UV-A) and emission in the visible region.



The 3D imaging is best understood in the context of the conservation treatment of the painting, which has been lined. Consequently, original features relating to stresses in the canvas due to stretching on the original secondary support and subtle differences due to the thickness of the paint layers have been flattened and regularised. A number of features may be specifically highlighted:

- Areas of impasto have been flattened, most likely as a result of prior lining treatment of the painting.
- There is notable distortion of the paint film around areas of impasto, visible as concave 'moating' deformation (sunken channels around raised areas), probably also as a result of prior lining treatment of the painting pushing these areas down.
- A horizontal crease across the entire width, roughly half-way up the painting (visible as having been retouched under UV light). This likely results from the painting having previously been folded.
- An area of 'rippling' (canvas distortions, cause unknown) near the right-hand side.
- Some minor bagging (an area of slack canvas) of the lower right-hand corner.
- The significance of horizontal deformation along the bottom edge of the painting is not clear.

### ***B.3.iii Short-wave infrared (SWIR)***

The interest in technologies capable of imaging artworks past the red end of the visible spectrum, in the 'near' ('NIR') or short-wave ('SWIR') infrared regions, has primarily developed out of the long-standing application to reflectography, exploiting the phenomenon of variable transparency of paint films at different wavelengths to enable visualisation of features lying beneath the surface. Imaging of underdrawing has been a major contribution to the study of authorship in paintings, permitting a fuller comprehension of artists' working practices and extending the evidence used in attribution questions. Practical experience (as well as theoretical consideration) has shown that deeper IR cameras can confer additional benefits in terms of penetration to underlying layers; consequently, a system capable of operating in the SWIR region was used here (see **Protocol 3.4**).

Due to the fragmentary aspect of the underdrawing, in charcoal, only small glimpses of this preparatory stage could be resolved in the SWIR (**Plates 6, 7**) though a general presence of charcoal fragments was observed over the painting when examined with magnification (**Plates 10.c, 11.a, 11.b**), which clearly relate to the process of setting in the forms. There also appears to be use of a thin, dilute paint used as a second stage of the laying in of the composition; such markings are likewise visible in the detailed images. The reason for the lack of resolution in IR lies in a number of factors, probably a combination of the thin and diffuse distribution of the material and the IR blocking properties of the thick overlying layers of paint

### ***B.3.iv X-radiography and weave analysis***

X-radiography shows internal structures in paintings because the transmitted X-rays are blocked to different degrees by virtue of the inherent absorption and thickness variations of the constituent materials. For example, pigments based on lead (such as ‘lead white’) stop the passage of X-rays more effectively than materials based on organic compounds (such as carbon blacks or the binding medium of the paint), while a thicker application of a material will block more than a thinner one. This allows visualisation of sub-surface features, such as abandoned or altered earlier phases (*pentimenti*), use of techniques such as superimposed forms as opposed to forms left in reserve, characteristic brushwork and so forth.

Here, the prepared surface of the canvas is largely covered by the application of paint, which extends to the tacking margins, although small areas of ground are visible throughout the painting where forms abut. Consequently, the X-ray (**Protocol 3.6; Plates 8, 12.b**) reveals a very direct rendition of form, with areas painted in reserve imaging brightly (where they block the passage of X-ray energy), and areas immediately around many of these forms appearing dark. The dark areas in the X-ray corresponding to the thinly primed areas of canvas that were left visible (i.e. unpainted; these are more X-ray transparent than heavily worked regions).

Infilling of the interstices of the threads comprising the canvas support with the priming (ground) also allows the canvas weave to be visualised in the X-ray. Even if a painting is lined, making direct access to the original canvas difficult or impossible, X-ray images can permit the primary weave structure to be examined in detail. A common characterisation of canvases (apart from weave type) is the ‘thread count’, or number of threads per unit in warp and weft directions. Conventionally determined by hand-measuring a number of representative areas, this is now done by applying an image processing algorithm to the entire X-ray image, which has the benefit of providing both greatly enhanced determination of thread counts as well as density and thread orientation information across the whole painting (see **Protocol 3.7; Plates 9.a-c**).

Here, the canvas was found to be a plain weave. The thread count on this work was determined 10.6 threads per centimetre in the vertical direction and 10.1 in the horizontal. The well-distributed and even cusping distortion at the left edge of the canvas only suggests that the format of the work has likely been trimmed or cut down somewhat along the other three sides (**Plate 9.a**).

## **C. Sampling and analysis**

### **C.1 Introduction**

Samples were taken of the support, ground preparation and paint layers of the work for analysis by different means in order to determine the range of materials (canvas, pigments, binders and coatings) used in the painting, the nature of the preparation layer and the sequence of layering employed in building up the painting (**Table App.1.i and Plate 13**).

To this end, a series of 11 locations selected over a representative range of the painting were micro-sampled for identification of the pigments (**Table App.2.i**), with six micro-samples of paint taken for analysis of the binding media (**Tables App.2.ii-2.iv**). Two further samples were taken for preparation as cross-sections to study the layering in the selected areas, with the aim of elucidating the development of the painting (**Plates 14-18**). Finally, canvas threads were taken for fibre identification and radiocarbon dating (**App.2.v, Protocol 2.7** and **App.2.vi, Protocol 2.8**).

Micro-samples for analysis were taken from locations that were adjudged to be original (that is, were clearly contiguous with those below and adjacent to them, and not retouching or repair). Locations were also further selected to represent as wide a range of the colours – and therefore probably pigments and media – as possible. Thus, the materials identified and discussed below therefore represent, as far as can be determined, the full extent of the original palette used by the artist.

The micro-samples taken for pigment characterisation were subjected to systematic analysis by polarised light microscopy (PLM) combined with UV-visible-near infrared micro-spectrophotometry, scanning electron microscopy-energy dispersive X-ray spectrometry (SEM-EDX), Raman microscopy and some Fourier Transform Infrared Spectroscopy-Attenuated Total Reflectance (FTIR; **App.2.i-2.ii, Protocols 2.1-2.4**).

Organic components were identified by FTIR (**App.2.ii, Protocol 2.4**) and subsequently by Gas Chromatography-Mass Spectrometry (GCMS; **App.2.iii, Protocol 2.5**). Protein staining of cross-sections using SYPRO<sup>®</sup> Ruby was also conducted (**App.2.iv, Protocol 2.6, Plate 16**).

All of the analytical techniques applied are standard methods within the field, capable of allowing the kinds of differentiation required for this type of work. Comparison was also made between samples from the painting and examples of similar pigments from a large collection of reference standards previously analysed by multiple means<sup>7</sup>. Certain differentiations cannot necessarily be made from this range of techniques, although for present purposes the level of discrimination is thought to be largely or wholly sufficient. All materials were generally identified through a combination of the techniques applied; however, certain key diagnostic features were specifically determined through one or other method.

## C.2 Support

The canvas was identified as being based on linen (*Linum usitatissimum* L.) in both weave directions (**App.2.v, Protocol 2.7**).

---

<sup>7</sup> The pigment reference collection belongs to the Pigmentum Project (see: <http://pigmentum.org>) and runs to around 3500 samples of both historical and modern origin. Analysis of this collection includes PLM and SEM-EDX as well as other techniques such as X-ray diffraction and Raman microscopy. Access to this research collection is gratefully acknowledged. Reference to specific specimens in the text of this report is to the Pigmentum collection number [Pxxxx]. An organic binding media reference collection is also held by AA&R; samples in this set are cited as [AARxxx].

### C.3 Radiocarbon dating

Radiocarbon dating was applied to linen fibres from the canvas support (**App.2.vi, Protocol 2.8**).

The radiocarbon date was determined as  $424 \pm 23$  years before present. After calibration, this yielded an anomalous date distribution for the painting giving ranges 1430-1490 and 1603-1609 at the 95.4% level. The reason for this result is unknown but most likely due to contamination of the sample such as incomplete removal of the *poly*(vinyl acetate) known to be present (as the adhesive for the lining).

### C.4 Ground

The very thin ground (Sample [1]; see also for an image in cross-section, **Plate 15**) was found to be composed of zinc oxide ('zinc white') bound with oil and some protein, possibly a casein emulsion with oil.

By FTIR the binding medium of the ground was found to consist of a drying oil and a proteinaceous compound. Very faint pink coloration in the white ground following staining with SYPRO® Ruby (**App.2.iv, Plate 16**) would support the determination of a minor component of protein in the ground layer and, additionally, phosphorus detected by EDX could suggest casein as an identification (**Table App.2.i, Sample [1]**).

### C.5 Underdrawing

The underdrawing material (Sample [12]) was identified as charcoal.

### C.6 Paint layers: Pigments

The following **pigments** (**Tables App.2.i, App.2.ii**) were identified in the paint:

- Lead carbonate hydroxide ('lead white')
- Lead sulfate ('lead white')<sup>8</sup>
- Zinc oxide ('zinc white')
- Barium sulfate (as a filler, not a primary pigment)
- Lead chromate ('chrome yellow')
- A yellow earth pigment containing goethite
- A red lake pigment (dyestuff not further identified), probably on an aluminium phosphate sulfate substrate
- Iron hexacyanoferrate(II) ('Prussian blue')
- Cobalt aluminium oxide ('cobalt blue')
- Ultramarine, synthetic (blue)
- A carbon-based black

---

<sup>8</sup> Present in two green samples with iron hexacyanoferrate(II) and lead chromate.

## C.7 Paint layers: Binding media

All paint samples analysed for binding medium using FTIR indicated the presence of a drying oil, determined by GCMS on two of the samples to be linseed (**App.2.ii-iii**).

FTIR also indicated the presence of metal soaps, probably of lead and zinc, assumed to be reaction products between pigments and binding medium (**App.2.ii**).

## C.8 Stratigraphy

The preparation of cross-sections allowed for examination of the overall stratigraphy and composition of the priming and paint layers.

In Sample [3] (**Plates 14-16**), taken from a largely yellow area, a full layer structure is preserved. The sample includes a large piece of canvas fibre, covered with a thin, irregular layer of the zinc white ground; no sign of an isolation layer (to seal the canvas before the zinc white was laid on) was observed. Above this is a dark blue paint layer, which intermingles with bright, chrome yellow paint, indicating a wet-in-wet technique or only summary mixing of colour on the palette.

In Sample [5], (**Plates 17, 18**), a sample of flesh paint from the figure, white forms the paint matrix while the colour is provided by streaks of pink paint, suggesting very summary mixing of colour. Here too, traces of the zinc white ground are present, but only in fragments at the base of the sample, right. These are best distinguished under UV illumination as the green luminescence of the zinc oxide pigment allows them to be resolved from the overlying pink layer consisting of lead white layer with deep red-pink swirls of red lake paint running through it. There are a number of larger, black particles in the white layer, probably fragments of charcoal underdrawing (see in particular, the horizontal particle, lowermost **Plate 18**).

As noted on the painting, there are no signs of complex layering, no translucent glazes; the composition has been worked in direct applications of paint.

## D. Discussion of the findings

### D.1 Support, ground and preparatory work

#### *D.1.i The support*

The painting has been executed on a coarse, plain-weave, linen canvas (**App.2.v, Plate 10**) with thread counts of 10.6 per cm in the vertical direction and 10.1 per cm in the horizontal direction (see **Plate 9**). The weave is quite tight, with only occasional, small interstices observed between the threads.

The canvas is of an extremely rough character, suggesting it is not of high quality. This is seen by the inclusion of many slubby and irregular threads (**Plate 10.c**) in both directions of the weave, as well as numerous bits of linen fibre husk (**Plate 11.a**), indicating that the plant

fibres were not carefully cleaned and homogenized before processing as threads. Due to the very loose spin of the individual threads, the canvas is distinctive in its ‘furry’ or ‘hairy’ appearance. Numerous bits of fibre stand proud of the threads. This creates the appearance of ‘hairs’ matted in the paint and ground surface (**Plates 11.a, 11.b**). The type of material is more consistent with those produced for domestic or industrial use, rather than canvas produced specifically for fine art painting.

The canvas is fully lined (**Plate 5**). It is affixed to a later (non-original) stretcher. As noted, tacking margins have been removed in the lining process, and the edges of the painting finished with brown paper tape (**Plates 5, 10.a, 10.b**).

Judging by the cusping (variable tension in the support caused by the pulling during stretching), which is clearly visible only along the left side of the painting, though faintly visible to the right, it may be speculated that the painting has changed slightly in format from its original dimensions (**Plate 9.a**). On this basis, one might conjecture that the painting was originally somewhat larger along the upper, lower and right sides. As the painting has been fully lined, no evidence for any original inscriptions or labels present on the verso survive; those which are present are of a later date<sup>9</sup>.

#### ***D.1.ii Priming***

The canvas has been primed with a white ground layer, applied to the stretched canvas by hand (i.e. it is not an industrially prepared canvas) (**Plates 10.b, 11.a, 11.b**). Its application is thin and irregular; it does not always fill the interstices and does not always cover canvas fully (**Plate 11.b**). This is evidenced in the cross-sections prepared from samples of the painting; in Sample [3] especially, the uneven nature of this layer is clearly seen (**Plates 14, 15**). The thickness of the white ground is proportionally much thinner than that of the overlying paint layers, even where it is at its thickest. It is composed of zinc oxide (‘zinc white’) mixed with what may be an oil and casein emulsion. The ground tests positively for oil (FTIR) and stains lightly positive for protein (**App.2.iv, Plate 16**). No evidence for an isolation layer (a glue or oil sealant applied to the canvas before the priming) was noted.

#### ***D.1.iii Underdrawing***

Examination of the painting under magnification revealed the presence of powdery black material along the outlines of the forms of the composition (**Plates 11.a, 11.b**). This material was judged likely to represent remains of the artist’s preparatory drawing and a sample was taken for analysis - Sample [12] – which was found to be charcoal. As charcoal is a friable, dry material, unlike paint, it does not have the advantage of a liquid medium to assist in adhering it to the surface. Consequently, the particles are held in place only tenuously; often it may be seen that they have been dragged into the paint as it was applied (see cross section 5, **Plate 18**, in which a large black particle is visible at the lower edge, and several other rounded black particles are visible in the body of the paint layers).

---

<sup>9</sup> These are described in more detail in Franken (2017a) *op. cit.*



Despite the known presence of an underdrawing and the use of high intensity short-wave IR imaging (SWIR) the underdrawing was not resolved in the IR image (**Plates 6, 7**). This phenomenon has been observed with increasing frequency in recent years as more and more late 19<sup>th</sup> and early 20<sup>th</sup> century paintings are studied with imaging techniques previously applied primarily to Old Masters. Careful study of such paintings, combined with IR imaging, has documented the common use of underdrawings in the works of many painters where they had not formerly been recognised; equally, these underdrawings, due to their friable nature (thus, easily disrupted and dragged by the paint when applied) and the nature of early 20<sup>th</sup> century paint (often based on heavy metals and applied very thickly), have been shown not to resolve in most infrared images<sup>10</sup>. The use of underdrawing in *Rusalka*, likewise, does not resolve clearly in infrared imaging; only small passages may be seen (**Plate 7**).

## D.2 Paint, pigments and binding media

### *D.2.i General observations*

The condition of the painting is generally quite good, although there is minor loss and flaking, especially along the central fold line (clearly visible in the UV and IR images: **Plates 2, 6**). As noted above, the painting has been lined and mounted on a new stretcher, its original dimensions possibly somewhat modified along the upper, lower and right edges.

Both the nature of the canvas and the ground might be seen in the context of an artist interested in working on a textured support, and/or, an artist wanting to save money on supplies. The canvas - likely a cloth made for domestic or industrial use, not as an artists' material - and the thin, irregular application of the ground which allows the fibrous nature of the support to remain visible may both have been a cheap solution in the provision of needed materials. Equally, as the ground is clearly applied by hand - this is not a factory prepared, ready to use painter's canvas - less cost was likely incurred through the choice to mix the zinc white and oil and applying the mixture as part of the process of creation. As the tacking edges no longer survive, one cannot be sure if the ground extended only to the edges of the picture plane or not.

The inclusion of slubby fibres and plant husks in addition to the fibrous surface of the canvas all provide the painter with a textured, irregular surface on which to work. Given the use of wide brushes, evident and vigorous brushstroke and little concern for smooth transitions or blending, these characteristics present a consistent aesthetic.

The painting is executed in a very sure and spontaneous manner, leaving areas of primed canvas exposed between the adjacent forms (see **Plates 8, 11, 12**)<sup>11</sup>. The use of an underdrawing must have facilitated this manner of working, with very few overlaps of colour

<sup>10</sup> This fact was first widely noted in the literature during the investigation of Impressionist paintings in the Wallraf Richartz Museum, Cologne, in 2010, during the course of the investigations for the exhibition *Impressionism: Painting in Light*. The phenomenon of friable underdrawing that does not resolve in IR images was observed in Monet's works.

<sup>11</sup> The use of reserves is very common in Goncharova's work. See Rioux, Aitken and Duval (1998) *op. cit.* pp. 19, 25, 26.



or form. No evidence for complex layering was seen; areas are worked quite directly, with mixing both on the palette, and wet-in-wet directly on the canvas. The colours are bright and intense, the paint strongly opaque and used quite thickly (**Plates 3, 4**) as well as spread thinly in other passages. The lining of the painting has evened off the local stresses that would have otherwise been present between paint and canvas, leaving a very flat, uniform surface, punctuated by the loaded impasto brushstrokes, perhaps slightly flattened by the process. It is likewise unclear to what degree the fibrous aspect of the surface has been regularised through the application of the lining. Though forms are mostly worked in reserve, the application of outlines, used in some areas and rendered in a variety of colours, formed the final steps in finishing the work (**Plate 12.c**). No use of transparent glazes was observed; the colours remain intense, though the surface aspect is quite matte. The painting does not show evidence of having been varnished, in keeping with the artist's preference for a brightly coloured, rough, matte finish. Due to the state of the painting (with edges covered by brown paper tape) it is not possible to observe to what extent the paint continued up to, or over, the turnover edges.

#### ***D.2.ii Paint: pigment and binding medium***

The painting displays a brittle crack pattern in the thicker regions of paint consistent with an oil painting of more than 100 years of age.

While zinc white was used for the ground, lead white appears have been the pigment chosen by the artist for the painting proper. Barium sulfate was found in a blue paint based on cobalt aluminium oxide, and apparently then as an additive to the paint formulation, as it does not occur elsewhere. Two tones of yellow (yellow earth and lead chromate) have been used and three blue tones (Prussian blue, cobalt aluminium oxide and synthetic ultramarine). No individual green pigment seems to have been used; rather, greens are created by mixtures of lead chromate and Prussian blue.

The cross-sections prepared confirm the observations made on the surface, and with the various forms of imaging: the paint was worked freely and directly (**Plates 14-18**). Mixing has taken place both on the palette, and on the brush, sometimes wet-in-wet directly on the canvas. This direct application has led to quite thin passages where the canvas weave and fibrous texture of the ground remain fully visible (**Plate 11.b**), and others where it is fully obliterated by a heavy build-up of impasto.

#### ***D.2.iii Materials analysis and implications for dating***

A date of 1908 is proposed for the painting based on stylistic grounds. Of the evidence collected, none of it speaks against the validity of this assessment. The radiocarbon result for the canvas was anomalous, probably due to sample contamination, and therefore has no implication for dating of the painting.

The materials identified in the painting (pigments and binding media) are compatible with the supposed date (although they also continued in use after that time) and therefore have no implication for dating of the painting. The findings generally agree well with the data

collected in the study of 45 paintings by Goncharova and Larionov in the collection of the Musée national d'art modern, Paris<sup>12</sup>.

Other technical characteristics arising from the larger review of the works of Goncharova and Larionov may also contribute to a fuller understanding of the relative dating of this painting in the future.

## E. Conclusions

The examination of the painting revealed a work that was created with great spontaneity, with a relatively limited palette of materials. The fibrous, textured aspect of the support, which is clearly visible in the paint layer as well, is particularly characteristic, and is reflected in style in the vigorous handling of the paint. The results of the examination have not found any evidence that would speak against the proposed date of the work, 1908.

---

<sup>12</sup> The combination of zinc white ground with lead white paint presents the single exception, in that the authors claim that only zinc white was used throughout the paintings by the two artists. Rioux, Aitken and Duval (1998) *op. cit.* p. 18.

## F. Acknowledgements

Art Analysis & Research would like to thank the following people for their contributions:

### Museum Ludwig

<b>Dr Yilmaz Dziewior</b>	Director, Museum Ludwig	
<b>Rita Kestring</b>	Deputy Director, Museum Ludwig	
<b>Petra Mandt</b>	Deputy Head of Conservation, Museum Ludwig	Project coordinator Paintings conservator

### Project Team, AA&R

<b>Dr Jilleen Nadolny</b>	Principal Investigator	Project management
<b>Dr Nicholas Eastaugh</b>	Chief Scientist	Materials and data analysis
<b>Bhavini Vaghji</b>	Senior Scientist	Materials analysis
<b>Francis Eastaugh</b>	Senior Imaging Engineer	Scientific imaging processing
<b>Dr Joanna Russell</b>	Scientist	Materials analysis

### Project Subcontractors

<b>Verena Franken</b>	Freelance paintings conservator, Cologne, Germany	Project coordinator, examination, documentation and archival research
<b>Patrick Schwarz</b>	Rheinisches Bildarchiv Köln, Cologne, Germany	Photographic documentation
<b>Prof. Hans Portsteffen, Andreas Krupa</b>	Department of Conservation, Cologne University of Applied Sciences, Germany	Capture of X-ray data
<b>Xavier Aure-Calvet</b>	Freelance imaging specialist, Bristol, UK	3D imaging capture and post processing
<b>Prof Haida Liang and team</b>	Nottingham Trent University, UK	Hyperspectral imaging
<b>Dr Irka Hadjas and team</b>	ETH/ Swiss Federal Institute of Technology, Zurich, Switzerland	Radiocarbon analysis

We would also like to extend our sincere thanks to the Peter and Irene Ludwig Foundation and to the RARP donors and to its board of trustees, without whose generosity and vision this project would not have been possible.

## G. Appendices

Standard protocols used by AA&R in the preparation of this report for sampling, materials analysis and imaging are listed in each subsection below and detailed in the appendices to the global summary report.











### App.1. Sampling and sample preparation

#### Protocols:

[P.1.1] Sampling




[P.1.2] Cross-sectional analysis

#### App.1.i Sampling

<b>Table App.1.i</b> Samples taken for analysis				
#	Colour	Description	Location <sup>13</sup>	Analysis
1		Ground, thin greyish	56/635	PLM, SEM-EDX, Raman, FTIR
2		White	707/236	PLM, SEM-EDX, Raman, FTIR, GC-MS
3		Yellow	291/970	PLM, SEM-EDX, Raman, FTIR, GC-MS, CSA, SYPRO <sup>®</sup> Ruby Staining
4		Yellow brown	111/83	PLM, SEM-EDX, Raman
5		Red, white	699/240	CSA
6		Crimson red	543/810	PLM, SEM-EDX, Raman
7		Mint green	732/455	PLM, SEM-EDX, Raman
8		Dark blue	97/915	PLM, SEM-EDX, Raman, FTIR
9		Bright blue	191/845	PLM, SEM-EDX, Raman
10		Dark green	458/1039	PLM, SEM-EDX, Raman, FTIR

<sup>13</sup> The coordinates in this column are given in millimetres, the measurements taken from the left edge of the picture, and from the lower edge of the picture.

**Table App.1.i** Samples taken for analysis

#	Colour	Description	Location <sup>13</sup>	Analysis
11		Light green	158/886	PLM, SEM-EDX, Raman, FTIR
12		Underdrawing, black	370/88	PLM, SEM-EDX, Raman
13		Fibre	748/1078	PLM, FTIR, C14

### App.1.ii Cross-sectional analysis

Results are shown in **App.5, Plates 14-18**

### App.2. Materials analysis summary results

#### Protocols:

- [P.2.1] Polarised light microscopy (PLM)
- [P.2.2] Scanning electron microscopy and energy dispersive X-ray spectrometry (SEM-EDX)
- [P.2.3] Raman microscopy
- [P.2.4] Fourier Transform Infrared Spectroscopy-Attenuated Total Reflectance (FTIR-ATR)
- [P.2.5] Gas Chromatography Mass Spectrometry (GCMS)
- [P.2.6] Cross-sectional protein staining with SYPRO<sup>®</sup> Ruby
- [P.2.7] Fibre Identification
- [P.2.8] Radiocarbon dating

### App.2.i SEM-EDX, Raman microscopy and PLM analysis

**Table App.2.i** Analytical results SEM-EDX, Raman Microscopy and PLM

#	Colour	SEM-EDX (elements)			Raman Microscopy (peaks, cm <sup>-1</sup> )	Identification
		Major	Minor	Trace		
1	Ground, greyish	Zn	-	Al, Si, P, S, K, Ca, Cr, Fe, Pb	438 (vw)	Zinc oxide
2	White	Pb	Al	-	1440 (vw), 1355 (vw, br), 1302 (vw), 1049 (m), 679 (vw), 410 (vw, br), 325 (vw), 108 (vs)	Lead carbonate hydroxide [P0864]
3	Bright yellow	Al, Pb	S, Cr	Si	1054 (w), 970 (vw), 841 (vs), 404 (vw), 377 (w), 360 (s), 338 (vw), 329 (w), 139 (vw), 108 (vw)	Lead chromate [P2238] Lead carbonate type white

**Table App.2.i** Analytical results SEM-EDX, Raman Microscopy and PLM

#	Colour	SEM-EDX (elements)			Raman Microscopy (peaks, cm <sup>-1</sup> )	Identification
		Major	Minor	Trace		
4	Yellow-brown	Si	Al, Fe	Mg, P, S, K, Ca, Co, Zn, Ba, Pb	548 (vw), 402 (vw), 303 (vw), 246 (vw), 146 (vw)	<b>Goethite</b> Aluminosilicate clay minerals
6	Crimson red	Al	P, S	Si, Ca, Zn, Pb	1294 (vw, br), 234 (w)	Organic red on Al/P/S substrate
7	Mint green	Pb	Al	Cr	2152 (vw), 2092 (vw), 1048 (vw), 528 (vw), 275 (vw), 117 (w)	Lead carbonate type white (main) <b>Prussian blue</b> Lead chromate (trace)
8	Dark blue	Fe	K	Mg, Al, Si, P, S, Ca, Cr, Zn, Pb	2149 (w), 2089 (vw), 1585 (vw, br), 1277 (vw, br), 941 (vw), 530 (w), 278 (w), 218 (vw), 114 (vw)	<b>Prussian blue</b> <b>Carbon-based black</b>
9	Bright blue	Al	Co	Na, Si, P, S, K, Ca, Ba, Pb	2154 (w), 2093 (vw), 1032 (vw), 1001 (vw), 986 (vw), 951 (vw), 690 (vw), 537 (w), 278 (w), 234 (vw), 215 (vw), 195 (vw)	<b>Prussian blue</b> <sup>14</sup> <b>Barium sulfate</b> Cobalt aluminium oxide (main)
10	Dark green <sup>15</sup>	S, Pb	Fe	Al, Si, K, Ca, Cr, Zn	2154 (m), 2092 (w), 946 (vw), 840 (vw), 599 (vw), 532 (m), 360 (vw), 278 (m)	<b>Prussian blue</b> <b>Lead chromate</b>
11	Medium green	Al	Cr, Fe, Pb	Si, S, Cl, K, Ca	2154 (w), 2092 (vw), 944 (vw), 840 (vw), 716 (vw), 533 (w), 277 (m), 225 (vw)	<b>Prussian blue</b> <b>Lead chromate</b>
12	Underdraw-ing (black with some white)	-	Na, Al, S, Zn	Mg, Si, P, Cl, K, Ca, Pb	1585 (w, br), 1323 (w, br)	<b>Carbon-based black, (charcoal)</b> Ultramarine Zinc oxide

<sup>14</sup> Iron was not identified in the SEM-EDX analysis.

<sup>15</sup> The green is a co-precipitate of lead chromate and Prussian blue, sometimes known misleadingly as 'chrome green'. This coprecipitated pigment is also present in Sample [11], but with additional Prussian blue also.

## App.2.ii Fourier Transform Infrared Spectroscopy-Attenuated Total Reflectance (FTIR-ATR)

Table App.2.ii Summary results from FTIR			
#	Colour	FTIR (peaks, cm <sup>-1</sup> )	Identification
1	Ground, greyish	3287 (m, br), 2956 (vw, sh), 2919 (m), 2851 (w), 1734 (m), 1645 (m), 1582 (vw, sh), 1576 (vw), 1564 (vw), 1556 (vw), 1539 (s), 1456 (m), 1434 (vw), 1410 (vw), 1399 (w), 1315 (vw), 1244 (vw), 1159 (w), 1096 (vw), 743 (vw), 721 (vw), 669 (vw), 650 (vw)	Protein Oil Metal soap formation, zinc-based <sup>16</sup> Metal soap formation
2	White	3534 (vw), 3336 (vw, br), 2955 (vw, sh), 2918 (w), 2849 (vw), 1734 (w), 1717 (vw), 1634 (vw), 1539 (vw, sh), 1520 (m), 1385 (vs), 1166 (vw), 1098 (vw), 1043 (vw), 928 (vw), 853 (vw), 767 (w), 725 (vw, sh), 677 (s)	Lead carbonate hydroxide [P0864] Oil Metal soap formation, presumably lead-based
3	Bright yellow	3357 (w, br), 2955 (vw, sh), 2918 (w), 2849 (w), 1733 (w), 1699 (vw), 1569 (w), 1456 (w), 1395 (m), 1160 (vw, sh), 1095 (s), 1067 (vw), 1051 (vw), 1042 (m), 970 (vw, sh), 851 (vw, sh), 833 (vw, sh), 821 (s), 721 (vw), 692 (vw), 675 (w), 625 (vw)	Lead chromate [P2238] <sup>17</sup> Lead carbonate type white Oil Metal soap formation, presumably lead-based
8	Dark blue	3293 (vw, br), 3252 (vw), 2954 (vw, sh), 2918 (w), 2850 (w), 2065 (vs), 1706 (m), 1602 (vw), 1456 (vw), 1411 (w), 1245 (vw), 1159 (vw), 1123 (vw), 1089 (vw), 1044 (vw), 982 (vw), 834 (vw), 786 (vw), 726 (vw)	Prussian blue Oil
10	Dark green	3258 (vw, br), 2954 (vw), 2917 (w), 2849 (w), 2086 (s), 1732 (vw), 1715 (vw), 1600 (vw), 1539 (vw), 1455 (w), 1435 (vw, sh), 1416 (vw, sh), 1394 (m), 1163 (s), 1026 (vs), 965 (w), 922 (w, sh), 873 (w, sh), 835 (s), 729 (vw), 720 (vw), 677 (w), 627 (s)	Prussian blue Lead chromate Lead sulfate Lead carbonate type white Oil <sup>18</sup> Metal soap formation, presumably lead-based
11	Medium green	3312 (w, br), 2921 (w), 2852 (w), 2087 (s), 1732 (m), 1705 (vw), 1540 (w), 1456 (w), 1396 (m), 1318 (w, sh), 1156 (vw, sh), 1089 (w, sh), 1046 (m), 850 (s), 823 (m), 721 (vw), 675 (w), 625 (w)	Prussian blue Lead chromate Lead sulfate Lead carbonate type white Oil Metal soap formation, presumably lead-based

<sup>16</sup> The peaks present in the sample spectrum matched the reference spectrum of zinc stearate, reference number AAR308. Zinc was identified in the SEM-EDX analysis.

<sup>17</sup> The reference spectrum of lead chromate consists of peaks corresponding to lead sulfate too. These peaks are also present in the sample spectrum which could suggest that the lead chromate is likely in the form of lead chromate sulfate or lead sulfate is present in the reference spectrum too. The SEM-EDX data of the sample showed high amounts of lead with minor amounts of chromium and sulfur.

<sup>18</sup> The characteristic peak of oil occurring at around 1160 cm<sup>-1</sup> was not observed in the spectrum due to the presence of lead sulfate whose peaks were masking this characteristic peak of oil however it is assumed that oil is present due to the formation of metal soaps.



### App.2.iii Gas Chromatography Mass Spectrometry (GCMS) Analysis

Table App.2.iii Summary results from GCMS					
Sample #	Hexadecanoic acid, methyl ester (C <sub>17</sub> H <sub>34</sub> O <sub>2</sub> )		Octadecanoic acid, methyl ester (C <sub>19</sub> H <sub>38</sub> O <sub>2</sub> )		Ratio
	Retention time, mins	Peak area	Retention time, mins	Peak area	
2	25.663	3.491 x 10 <sup>9</sup>	29.605	1.936 x 10 <sup>9</sup>	P/S = 1.80
3	25.670	7.551 x 10 <sup>9</sup>	29.613	3.757 x 10 <sup>9</sup>	P/S = 2.01

The P/S value of **Sample [2]**, white paint, was 1.80, consistent with **linseed oil**.

The P/S value of **Sample [3]**, bright yellow paint, was 2.01, consistent with **linseed oil**.

### App.2.iv Protein staining with SYPRO® Ruby

Table App.2.iv SYPRO® Ruby stain results for 955.B, sample [3]				
Layer	EDX	FTIR	SYPRO® Ruby stain	Interpretation
Ground	<b>Zn</b> Al, Si, P, S, K, Ca, Cr, Fe, Pb	Peaks for protein and oil	Faint pink coloration in white ground	Probable presence of protein in ground layer. Phosphorus may suggest casein.
Paint	<b>Al, Pb</b> S, Cr, Si	Oil in white, bright yellow, dark blue	Dark blue too dark to tell if stained. Yellow layer does not appear to be stained.	No protein evident in paint layers

### App.2.v Fibre Identification of the Canvas

Table App.2.v Canvas fibre identification		
Sample	Observations under PLM	Interpretation
13v	Nodes across fibres, parallel extinction, S-twist Possible oxalate cluster, n<1.66	Bast fibre, probably linen ( <i>Linum usitatissimum</i> L.)
13h	Nodes across fibres, parallel extinction, s-twist A few structures with low birefringence appearing grey under crossed-polars, some with regular pattern of pitting consistent with wood	Bast fibre, probably linen ( <i>Linum usitatissimum</i> L.) Fragments of plant husk

## App.2.vi Radiocarbon measurement

Radiocarbon dating is a method for determining age estimates of formerly living organic materials<sup>19</sup>. Carbon has three naturally occurring isotopes,  $^{12}\text{C}$ ,  $^{13}\text{C}$  and  $^{14}\text{C}$ . Both  $^{12}\text{C}$  and  $^{13}\text{C}$  are stable, but  $^{14}\text{C}$  decays by very weak beta decay to nitrogen ( $^{14}\text{N}$ ) with a half-life of approximately 5,730 years. While alive, organic materials continue to exchange carbon with the environment, such that they are in equilibrium. On death, the  $^{14}\text{C}$  component begins to decay, such that over time the relative amount decreases. Measuring the level of  $^{14}\text{C}$  remaining in the material then allows for a date to be estimated. This must be additionally calibrated against natural historical variation in relative  $^{14}\text{C}$  levels in the environment, for which there are accepted standard curves expressing the changes over time<sup>20</sup>.

Prior to radiocarbon measurement, fibre identification was undertaken and the canvas sample was pre-tested using FTIR to ascertain the presence of any contaminating material that could influence the outcome. As noted elsewhere, the fibre was identified as a bast type, probably linen (*Linum usitatissimum* L.). FTIR indicated the presence of *poly*(vinyl acetate), and a proteinaceous material, in addition to the cellulose of the fibre<sup>21</sup>.

The canvas sample was then submitted to the Laboratory of Ion Beam Physics, ETHZ at the Swiss Federal Institute of Technology (*Eidgenössische Technische Hochschule Zürich*) for radiocarbon dating (see **Protocol 2.8**).

Table App.2.vi.i Radiocarbon measurement										
Sample-	Sample	Material	C14 age	$\pm 1\sigma$	F14C	$\pm 1\sigma$	$\delta\text{C}13$	$\pm 1\sigma$	mg C	C/N
Nr.	Code		BP				‰			
ETH-77068	AAR0955.B.13	Textile fibre	424	23	0.9486	0.003	-24.2	1	1	158.8

The radiocarbon date was determined as 424 years b.p.  $\pm 23$  years. After calibration, this yielded an anomalous date distribution for the painting giving ranges 1430-1490 and 1603-1609 at the 95.4% level. The reason for this result is unknown but most likely due to contamination of the sample such as incomplete removal of the *poly*(vinyl acetate) known to be present.

<sup>19</sup> Based on from the websites of the NDT Resource Center, <http://www.ndt-ed.org/EducationResources/CommunityCollege/Radiography/Physics/carbondating.htm> and the website of the Oxford Radiocarbon webinfo site: <http://c14.arch.ox.ac.uk/embed.php?File=webinfo.html>, both consulted on 3 February 2013.

<sup>20</sup> For example, that used here is one known as IntCal13.

<sup>21</sup> Non-cellulosic materials are aimed to be removed by the sample pre-treatment process prior to the radiocarbon measurement.

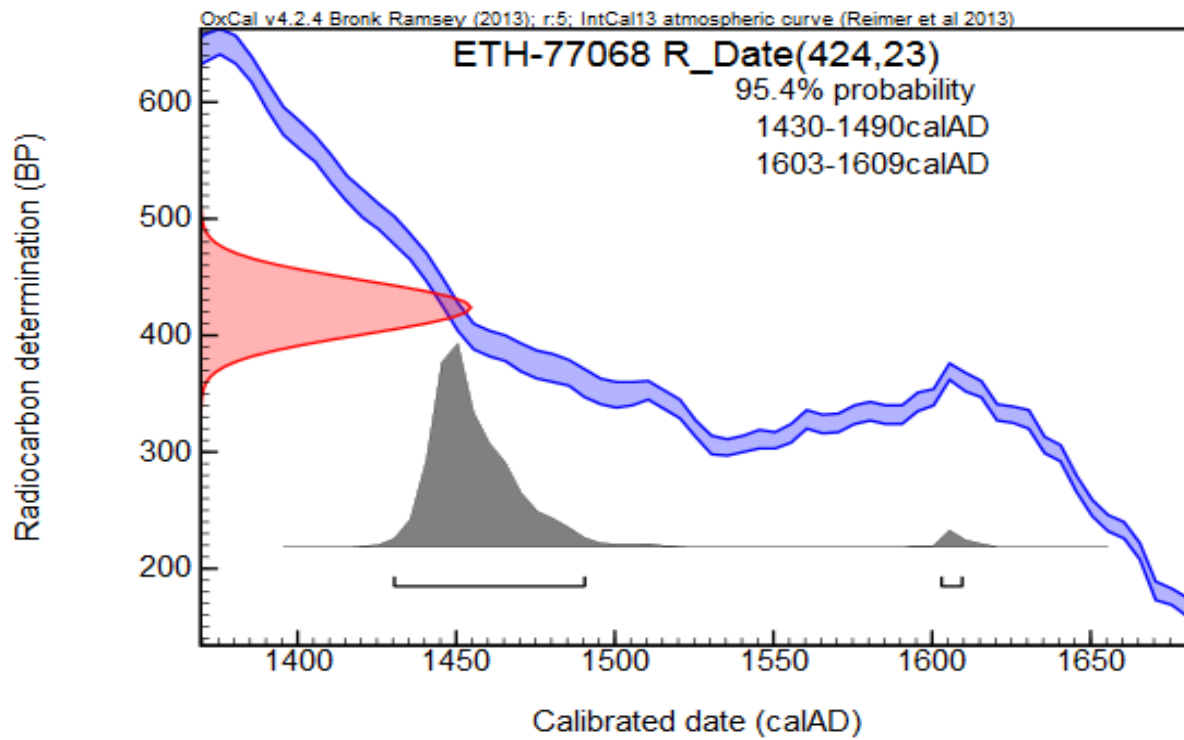


**Figure App.2.vi.ii** Radiocarbon determination.



### **App.3. Imaging methods**

#### **Protocols:**

- [P.3.1] Photography with visible light
- [P.3.2] Photography with ultraviolet illumination
- [P.3.3] 3D laser surface mapping
- [P.3.4] SWIR infrared imaging (IR)
- [P.3.6] X-radiography (X-ray)
- [P.3.7] Thread counting and weave analysis

**App.4. Plates**

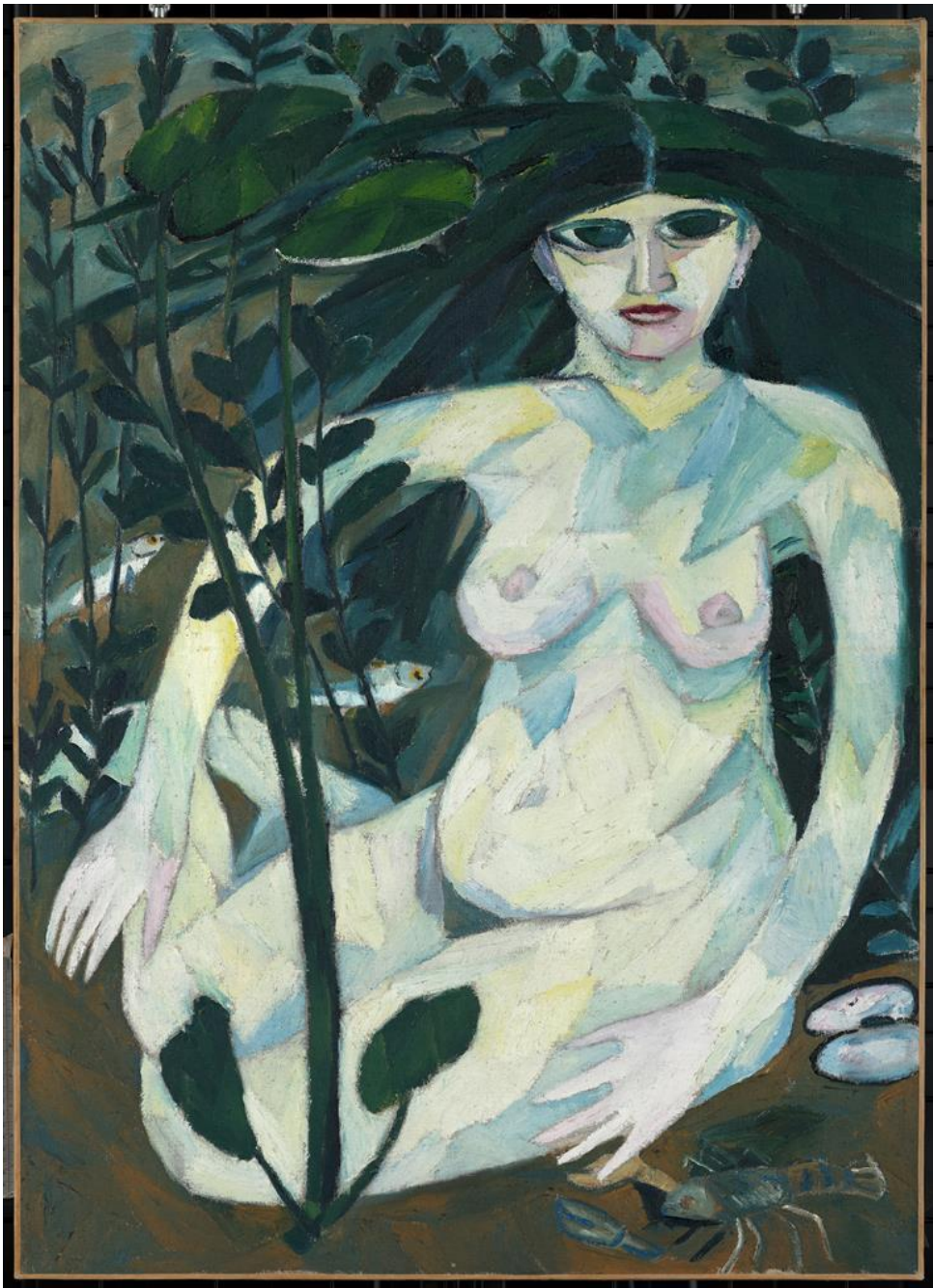


**Plate 1.** Natalia Goncharova, *Rusalka*, 1908, collection Museum Ludwig: Inv. Nr. ML 1304.  
**Recto, visible light.**

Rheinisches Bildarchiv Köln, Patrick Schwarz, rba\_d050881\_06, [www.kulturelles-erbe-koeln.de/documents/obj/05020006](http://www.kulturelles-erbe-koeln.de/documents/obj/05020006)





**Plate 2.** Natalia Goncharova, *Rusalka*, 1908, collection Museum Ludwig: Inv. Nr. ML 1304. **Recto, UV light.**

Rheinisches Bildarchiv Köln, Patrick Schwarz, rba\_d050881\_05, [www.kulturelles-erbe-koeln.de/documents/obj/05020006](http://www.kulturelles-erbe-koeln.de/documents/obj/05020006)



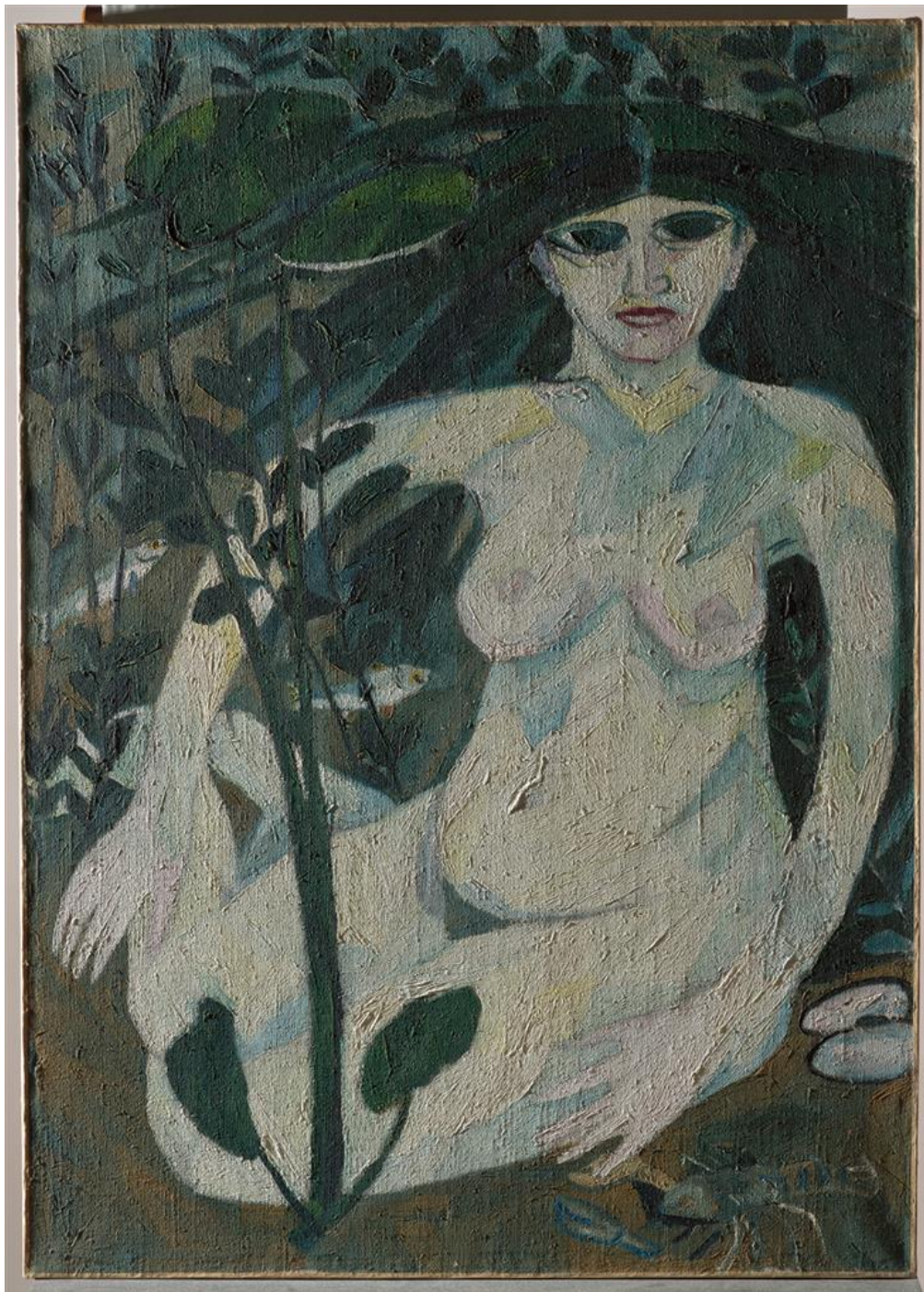


**Plate 3.** Natalia Goncharova, *Rusalka*, 1908, collection Museum Ludwig: Inv. Nr. ML 1304.  
**Recto, raking light.**

Rheinisches Bildarchiv Köln, Patrick Schwarz, rba\_d050881\_04, [www.kulturelles-erbe-koeln.de/documents/obj/05020006](http://www.kulturelles-erbe-koeln.de/documents/obj/05020006)



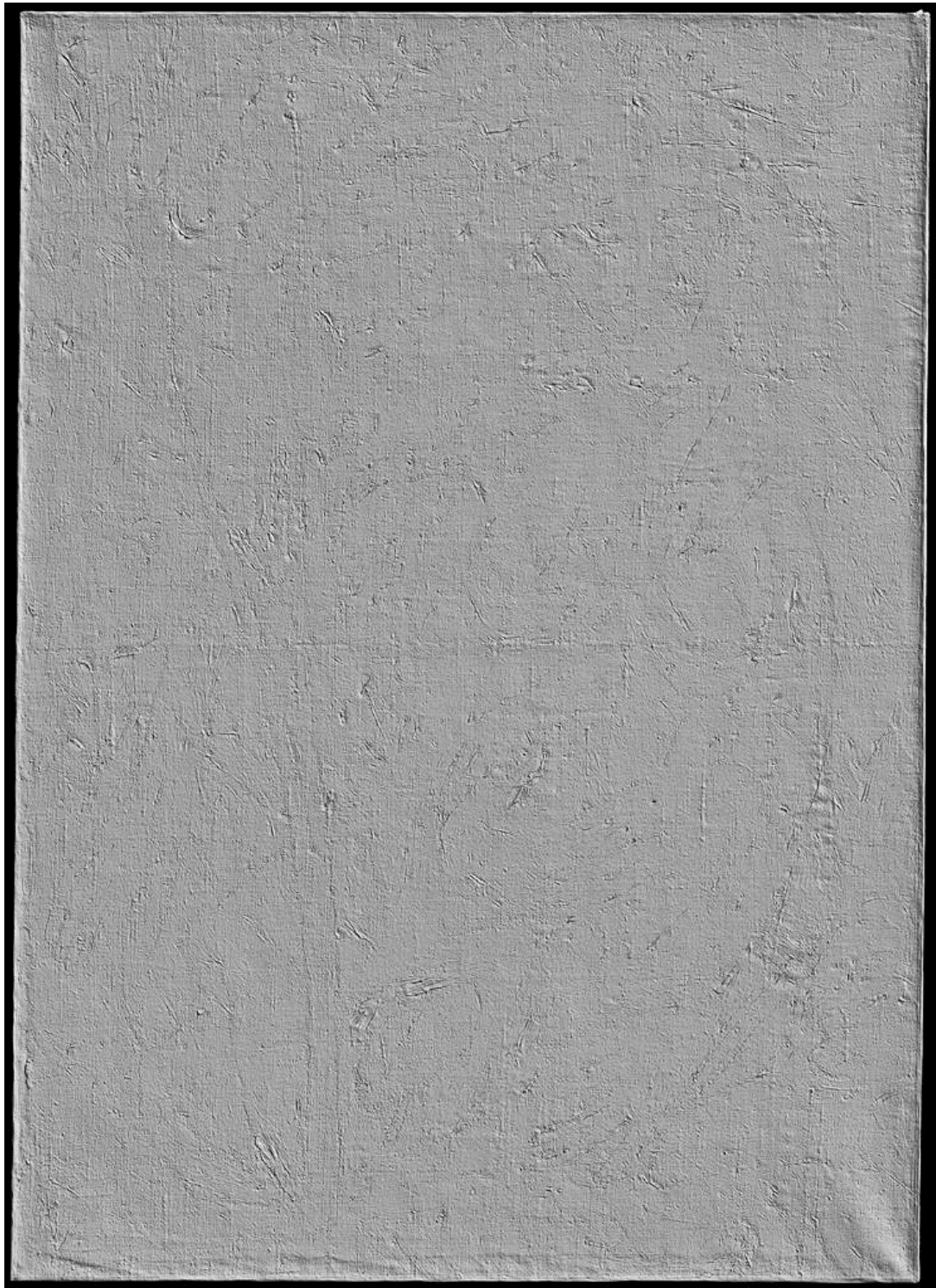


**Plate 4.** Natalia Goncharova, *Rusalka*, 1908, collection Museum Ludwig: Inv. Nr. ML 1304. **Recto,** 3D laser scan.



**Plate 5.** Natalia Goncharova, *Rusalka*, 1908, collection Museum Ludwig: Inv. Nr. ML 1304. **Verso, visible light.**

Rheinisches Bildarchiv Köln, Patrick Schwarz, rba\_d050881\_02, [www.kulturelles-erbe-koeln.de/documents/obj/05020006](http://www.kulturelles-erbe-koeln.de/documents/obj/05020006)



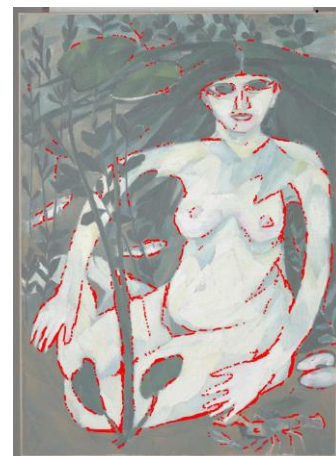
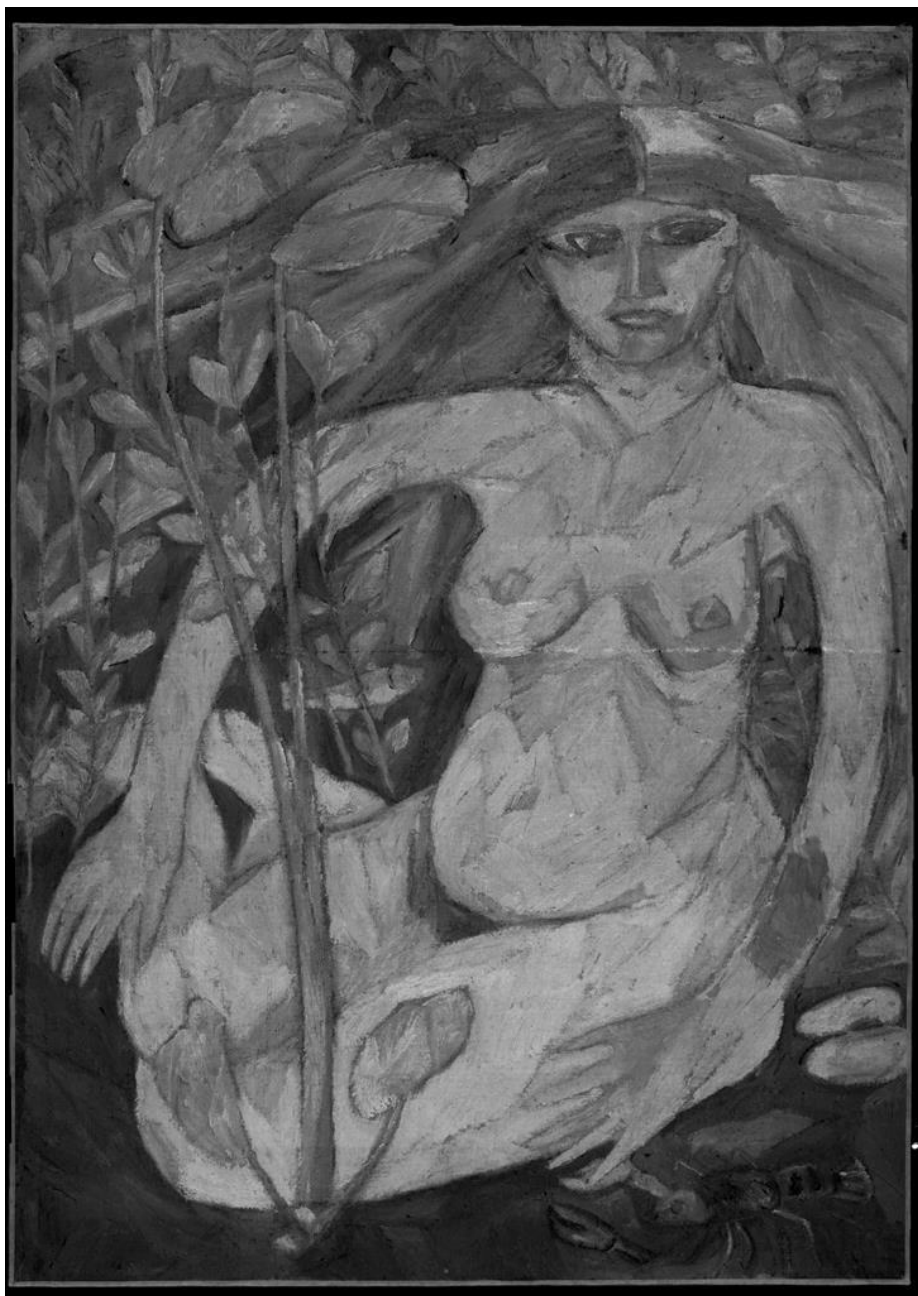


**Plate 6.a** Natalia Goncharova, *Rusalka*, 1908, collection Museum Ludwig. Image showing the observed extent of the charcoal underdrawing, as seen under the microscope.

**Plate 6.** Natalia Goncharova, *Rusalka*, 1908, collection Museum Ludwig: Inv. Nr. ML 1304. **Recto, SWIR image.**



**Plate 7.** Natalia Goncharova, *Rusalka*, 1908, collection Museum Ludwig: Inv. Nr. ML 1304. **Recto**, detail of SWIR image, contrast heightened.





**Plate 8.** Natalia Goncharova, *Rusalka*, 1908, collection Museum Ludwig: Inv. Nr. ML 1304. **X-ray image.**

Above, right, the image before digital compensation for the stretcher bars.

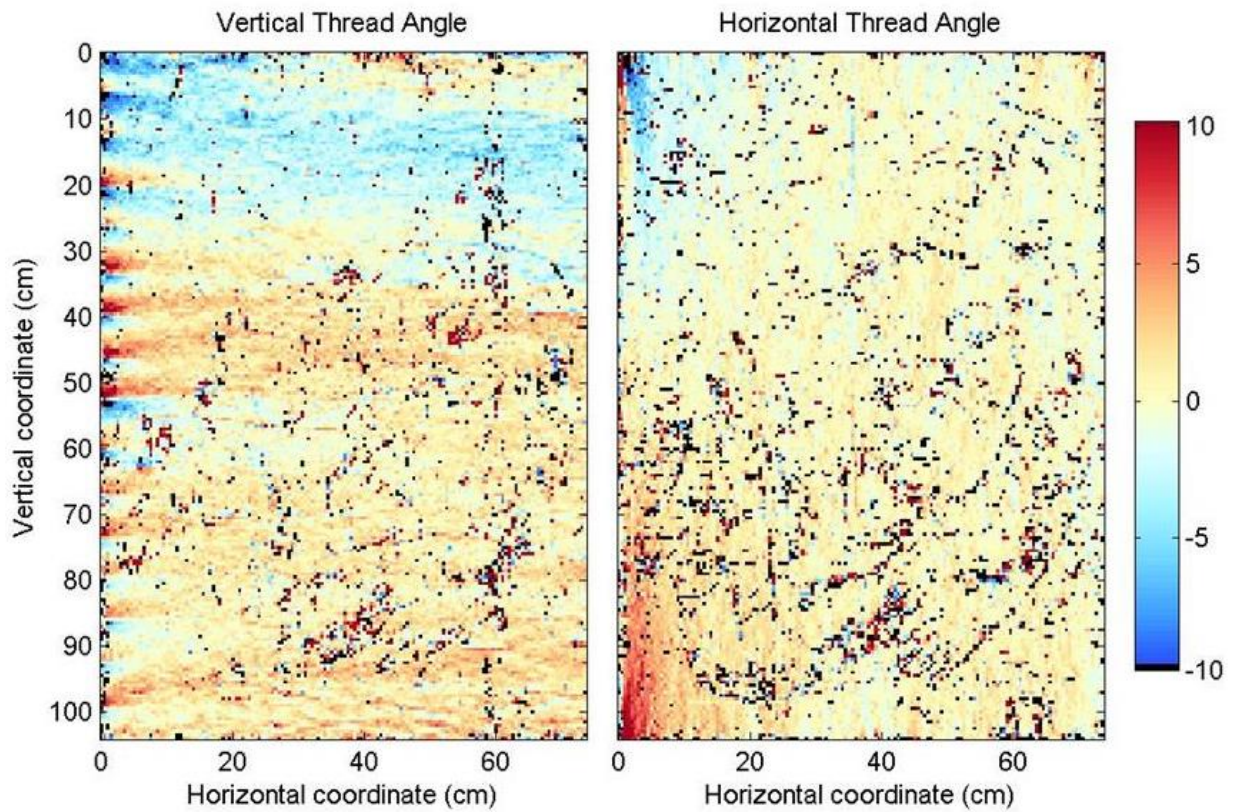


**Plate 9.a** Maps showing variation in canvas thread angle.

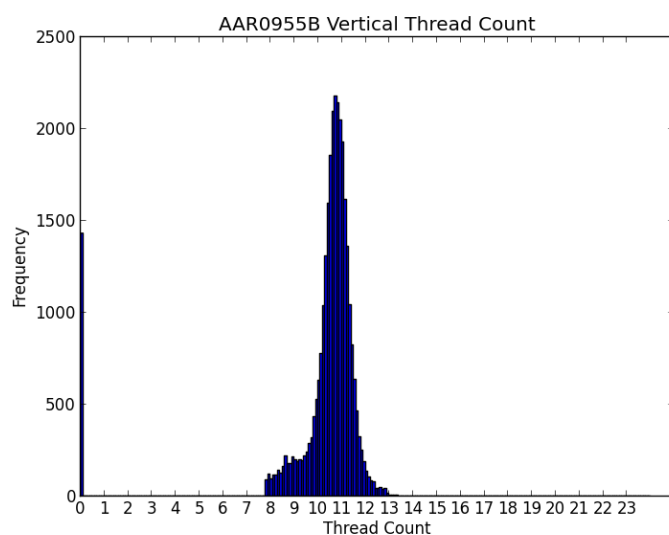


**Plate 9.b** Histogram of vertical thread count readings.

Showing variation in thread count per centimetre.

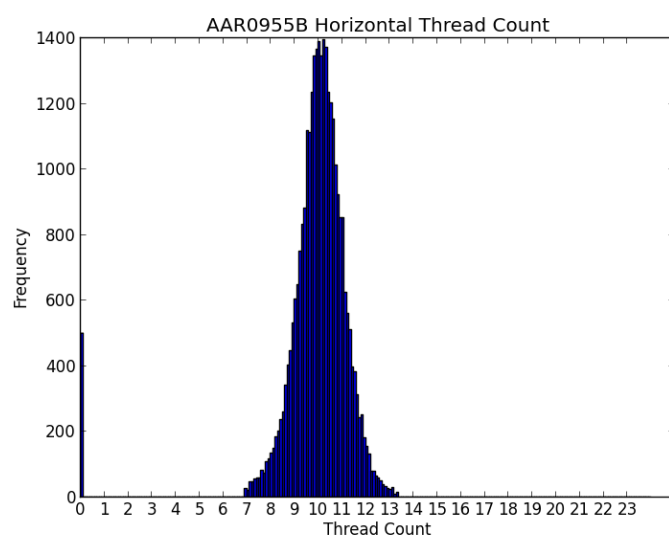


**Plate 9.c** Histogram of horizontal thread count readings.

Showing variation in thread count per centimetre.

**Plate 9.d** Table of thread count data (threads per centimetre)

	Mean	Estimated thread count (mode)
Vertical	10.6	10.7
Horizontal	10.1	10.2



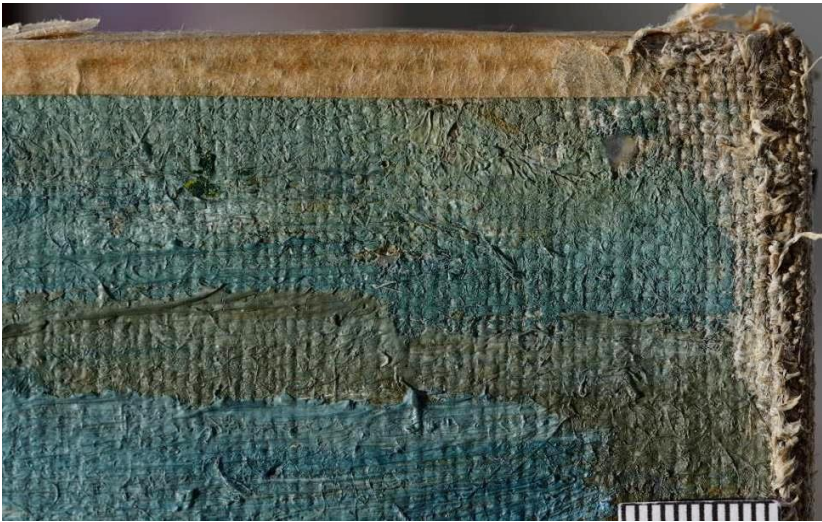


**Plate 10.a** Detail of canvas, recto, showing the exposed tabby weave canvas, upper right corner.

The canvas fibre a bast type, probably flax, with inclusions of flax husk. The canvas is lined, and paper taped around the edges.



**Plate 10.b** Detail of the primed canvas.

The thinness of the priming is clear; the fibres of the threads remain distinct giving the surface a 'furry' aspect.



**Plate 10.c** Detail of the canvas, recto, showing an example of the irregular thread inclusions.





**Plate 11.a** Microscopic detail of the underdrawing material.



**Plate 11.b** Microscopic detail recto; thin ground and underdrawing, loose fibres.



**Plate 11.c** Microscopic detail of paint, showing plant husk fragments from the canvas.





**Plate 12.a** Detail of the underdrawing material.

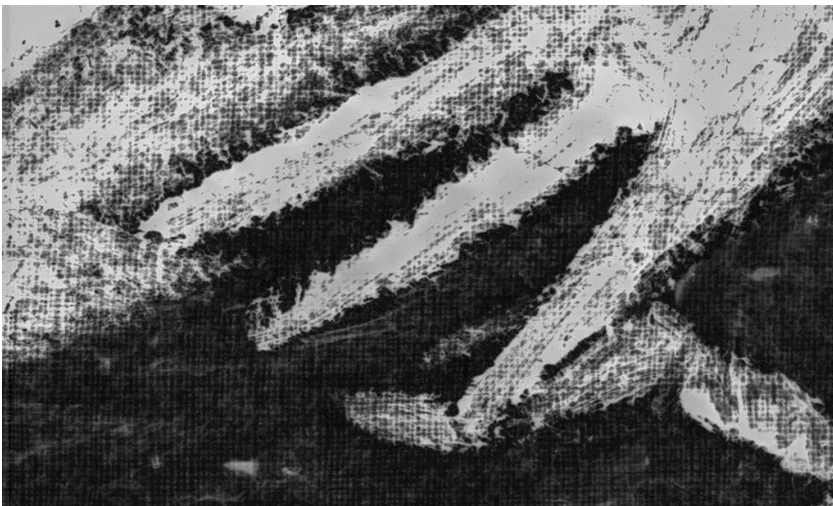


**Plate 12.b** Detail X-ray image, as 11.a.

The light tones, thickly painted in lead white, show as bright areas, while the exposed areas of primed canvas are the darkest.

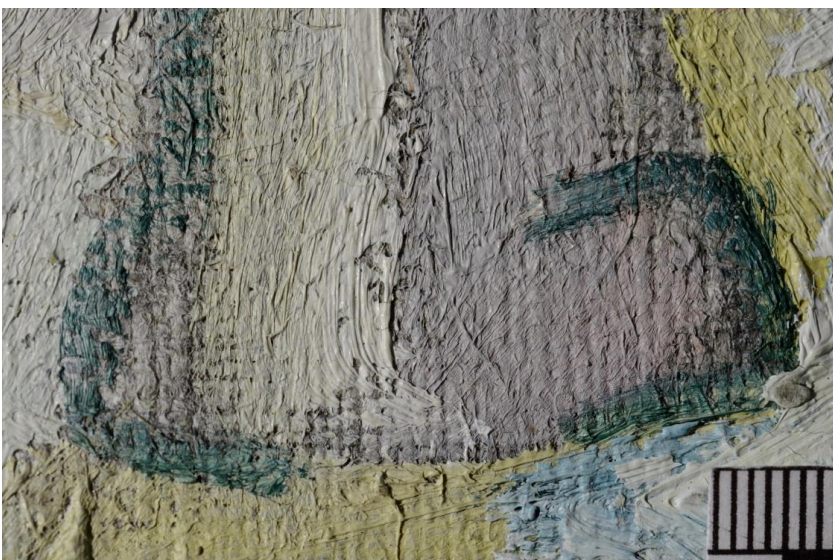


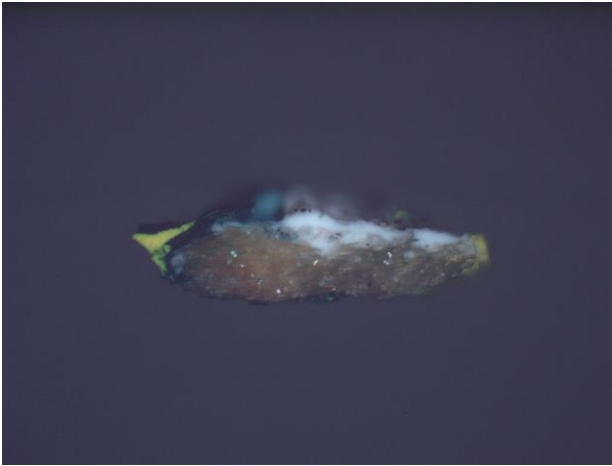
**Plate 12.c** Detail of paint, showing contouring of form in green (nose).





**Plate 13.** Image showing approximate location of samples taken for materials analysis.

## App.5. Cross-sections<sup>22</sup>



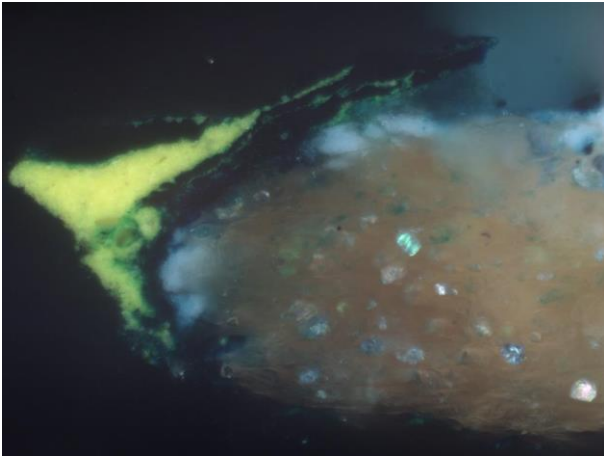
a.



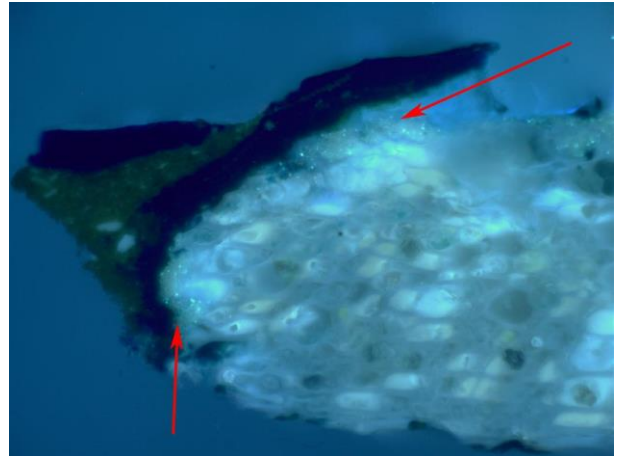
b.

### Plate 14. Cross section, Sample [3].

Image ~1mm high. The sample includes a large piece of canvas fibre, covered with a white fragmentary ground layer. Above this is a dark blue paint layer, which intermingles with a bright yellow layer.



a.

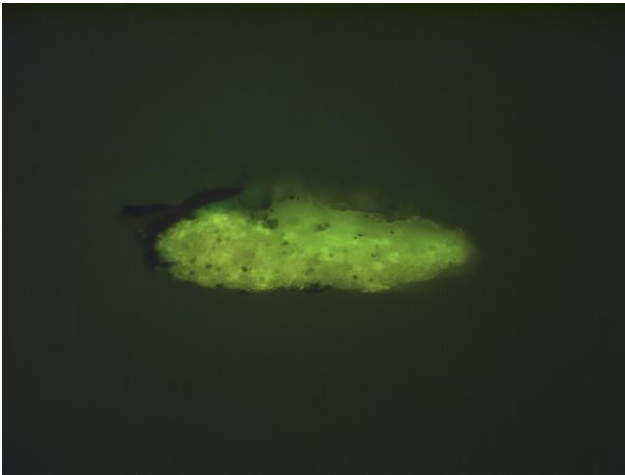


b.

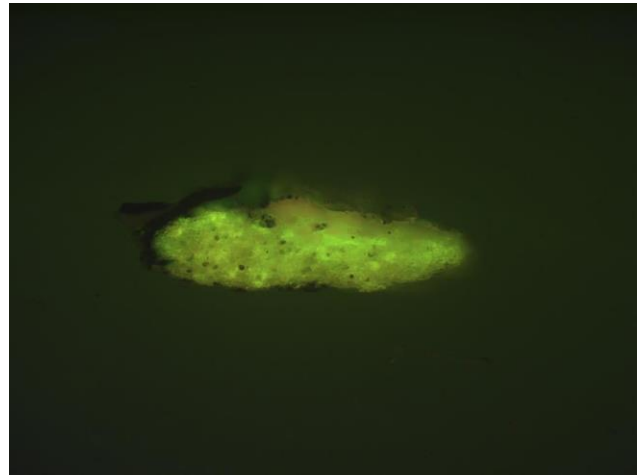
### Plate 15. Cross section, Sample [3].

Image ~260µm high. Yellow sample shown at higher magnification. The red arrows (in the UV image, right) point to the areas of white ground, within which some fine particles display a bright green luminescence in UV, indicating the presence of zinc oxide.

<sup>22</sup> Photographed under visible light, left (a.), and with ultraviolet illumination, right (b.) unless otherwise stated.



**a.**



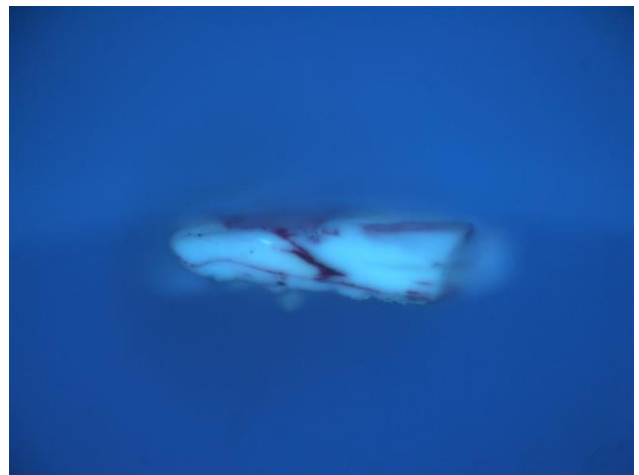
**b.**

**Plate 16.** Cross section, Sample [3], stained with SYPRO® Ruby.

Image ~1mm high viewed with Leica I3 filter before (left) and after (right) staining. Faint pink coloration in white ground, supports the presence of protein in the ground layer, which would confirm results by FTIR. Additionally, phosphorus detected by EDX may suggest presence of casein. In the paint layers, the dark blue was too dark to tell if staining had occurred despite the use of a fluorescent marker. The yellow layer does not appear to be stained.



**a.**

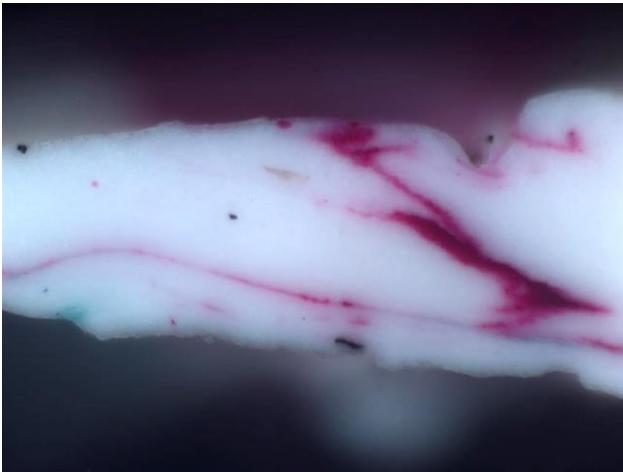


**b.**

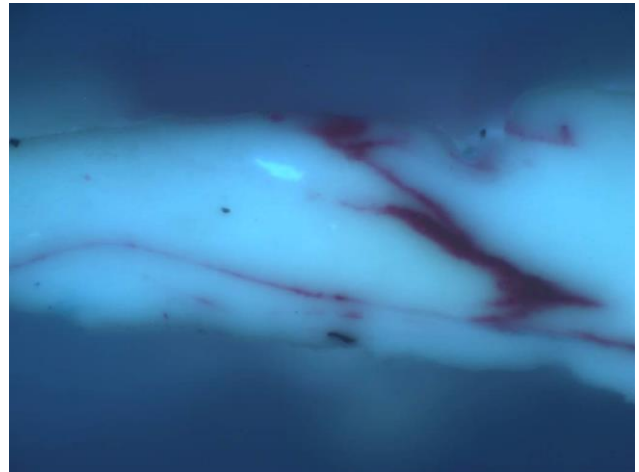
**Plate 17.** Cross section, Sample [5].

Image ~1mm high. Red-white from flesh. Traces of ground at the base of the sample, right, are visible due to the green luminescence of the zinc oxide pigment in UV. The paint layer is mainly white, with deep red-pink swirls of paint running through it.





**a.**



**b.**

**Plate 18.** Cross section, Sample [5].

Image ~260µm high. Red-white sample at higher magnification, showing the red-pink swirls more clearly, and one green particle at the base of the sample.